agriculture

MDPI

Study Protocol

Study on the Fragrant Pear-Picking Sequences Based on the Multiple Weighting Method

Wenhong Ma [1], Zhouyang Yang [1], Xiaochen Qi [1], Yu Xu [1], Dan Liu [1], Housen Tan [1], Yongbin Li [2,*] and Xuhai Yang [1,3,4,*]

1 College of Mechanical and Electrical Engineering, Shihezi University, Shihezi 832003, China; 20212009027@stu.shzu.edu.cn (W.M.); yangzhouyang@stu.shzu.edu.cn (Z.Y.); qixiaochen@stu.shzu.edu.cn (X.Q.); xuyu@stu.shzu.edu.cn (Y.X.); liudan01@stu.shzu.edu.cn (D.L.); tanhousen@stu.shzu.edu.cn (H.T.)
2 College of Water & Architechtural Engineering, Shihezi University, Shihezi 832003, China
3 Key Laboratory of Northwest Agricultural Equipment, Ministry of Agriculture and Rural Affairs, Shihezi 8832003, China
4 Xinjiang Production and Construction Corps Key Laboratory of Modern Agriculture Machinery, Shihezi 832003, China
* Correspondence: yishui-qingshen@163.com (Y.L.); yxh_513@shzu.edu.cn (X.Y.); Tel.: +86-15026232711 (Y.L.); +86-13899521305 (X.Y.)

Abstract: The production of the Korla fragrant pear is significant, but the optimal harvesting time is short; therefore, the reasonable use of mechanical arms for harvesting is conducive to promoting the sustainable development of the fragrant pear industry. The efficiency of a robot arm when picking fragrant pears is not only determined by the successful extraction of fragrant pears in a complex environment, but the picking sequence of fragrant pears also directly affects the efficiency of the robot arm. In order to simulate an orchard-picking scenario, this paper built three fragrant pear tree models indoors. The number of fragrant pears on the fragrant pear trees was 5, 10, and 20. Three sets of experiments were designed for comparison with real-world conditions. The main steps were as follows: calibrate the three-dimensional coordinates of each fragrant pear on the fragrant pear trees; determine the end position of the robotic arm at each picking point; find the inverse solution for each group; transform the solutions into matrix form using the rated power of each joint as the weight, and identify the minimum value, which is the angle of each joint in the robotic arm when picking the fragrant pear; use the intelligent socket to find the average energy consumption and average time consumed for picking each group of fragrant pears; and determine the loss ratio of the robotic arm based on the amount of rotation in each joint during picking. The experimental results show that the multiple weighting method reduced the energy consumption by 10.627%, 16.072%, and 24.417%, and the time consumption by 11.988%, 14.428%, and 22.561%, respectively, relative to the hybrid ant colony–particle swarm optimization algorithm, which proves the rationality of the fragrant pear picking order delineated using the multiple weighting method.

Keywords: picking sequence; drop point; multiple weighting; energy time consumption; loss ratio

Citation: Ma, W.; Yang, Z.; Qi, X.; Xu, Y.; Liu, D.; Tan, H.; Li, Y.; Yang, X. Study on the Fragrant Pear-Picking Sequences Based on the Multiple Weighting Method. *Agriculture* **2023**, *13*, 1923. https://doi.org/10.3390/agriculture13101923

Academic Editor: Jacopo Bacenetti

Received: 1 July 2023
Revised: 24 July 2023
Accepted: 28 July 2023
Published: 30 September 2023

1. Introduction

According to the latest data released by the Department of Agriculture and Rural Affairs of the Xinjiang Uyghur Autonomous Region, from 2018 to 2022, the brand value of Xinjiang Korla fragrant pears grew from CNY 9.888 billion to CNY 16.12 billion, as shown in Figure 1, with a growth rate of 63.03%. Its huge economic value has resulted in the fragrant pear planting area increasing year by year; by the end of 2022, Bazhou had a fragrant pear planting area of 489,600 mu, an output of 386,400 tons, and a fruit output value of nearly CNY 2.6 billion [1]. Combined with market demand, the best harvesting date for fragrant pears is from 21 to 26 September every year [2]. Short harvesting times, a large workload, and a labor shortage have resulted in many difficulties for growers and have also hindered the sustainable development of the fragrant pear industry.

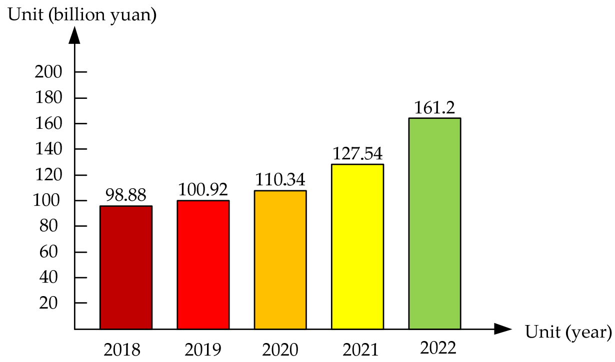

Figure 1. Korla fragrant pear brand value.

At present, the core of the fragrant pear industry is ensuring harvesting in the picking period with the lowest cost and the shortest time in order to solve the fragrant pear picking problem. The fragrant pear-picking order needs to be determined in order to solve this problem. The optimal picking sequence problem is a classical operations research problem that involves many subject areas. In the 1950s, the American mathematician Dantzig first proposed the use of linear programming to solve the picking sequence problem. Then, the first Japanese picking arm called the "fruit-picking robot" was developed in 1970, and many scholars conducted in-depth research on the picking sequence of the robot arm. The authors of [3] focused on the mechanism of competition, the use of k-means, open-source projects, and the Hough gradient detection algorithm for phase-out screening to determine the fruit-picking order. The authors of [4] solved the picking order of green peppers using the particle swarm algorithm to obtain the optimal solution using iteration. The authors of [5] combined vision and virtual reality for simulation experiments on collision-proof grape cluster picking sequences. The authors of [6] used the MATLAB-based lossless picking path planning approach, where picking started from the outside and moved inside, to solve kiwi-picking sequence problems. The authors of [7] used a neural competition mechanism based on the "winner-takes-all" neural competition mechanism, combined with area, distance, and saliency weighting strategies, to determine the order of apple picking. In an orchard, the robotic arm is powered by a battery, so the energy consumption of the arm needs to be considered while studying picking sequences. In order to extend the working time of a robotic arm and improve its picking efficiency under a limited energy supply, the principle of minimum energy consumption was used to determine the picking sequence of fruit. Research on the minimum energy consumption of robotic arms falls into two main categories, one of which is the optimization of the robotic arm as a whole, with the end-effector optimized for all fruit in Cartesian space. Fragrant pear-picking sequences are planned as a combinatorial optimization NP problem, i.e., the traveler's problem (TSP). Algorithms for the TSP problem fall into three main categories. The first is the intelligent method, consisting of the ant colony algorithm, genetic algorithm, particle swarm algorithm, simulated annealing algorithm, artificial bee colony algorithm, gray wolf algorithm, and others. The second is the approximate processing method, consisting of the double-spanning tree algorithm, greedy algorithm, and improved circle algorithm. The third is the exact method, mainly consisting of the exhaustive method and the dynamic planning method. When performing a picking task, the algorithm used to solve the fruit-picking sequence problem and find the shortest path is the TSP [8–13]. The second is in the joint space of the robot, arming each joint as a motor unit, with the power or torque calculated using the best pose [14–19]. Compared with the intuitive nature of TSP applied to large robotic arms, the use of weighting coefficients can be applied to all kinds of robotic arms with all the characteristics of the motion chain of robotic arms, which is more in line with the application of robotic arms in fragrant pear picking.

Accordingly, in this paper, we fully explained the planting method for fragrant pear trees in a fragrant pear garden, the physical characteristics of fragrant pears, and the structure of the robotic arm. Then, a placement point was added on the basis of "joint angle twice weighting" for the quality grading of fragrant pears. The picking process involved three stages, namely, the pre-picking origin, the picking point, and the drop-off point. After weighing the robot arm three times, the matrix was used to obtain the minimum weighted value of each fragrant pear and to propose the principle of "big in big" in the picking process. After using the hybrid ant colony−particle swarm optimization algorithm to solve the TSP shortest path, the energy loss and picking time of the two methods were measured using an energy consumption meter. After the picking task was completed, the loss ratio of the inner and outer rotors of each joint in the robot arm was determined according to the rotation amount for each joint, thus facilitating the maintenance and servicing of each joint of the robot arm, extending the working time of the robot arm, and reducing the picking cost.

2. Selection of a Working Object and Robot Arm

The planting method for fragrant pear trees in fragrant pear gardens, the physical characteristics of fragrant pears, and the structure of a robotic arm form the basis for studying the sequence of fragrant pear-picking using a robotic arm.

2.1. Characteristics of the Fragrant Pear Tree

The Korla fragrant pear tree has a straight trunk and tall crown, and the crown is a conical or natural semicircle shape. Because of the different cultivation and planting methods for fragrant pear trees, the height of the tree, trunk height, and crown are also different. After reviewing the information and visiting the orchard, the planting pattern was divided into two types: 3~4 m × 5~6 m for medium-density planting and 6 m × 6 m or 6 m × 7 m for regular thinning. Most growers use medium-density planting, so the first planting pattern was used as the basis for this study. The basic structure of the fragrant pear trees planted at medium density was as follows: 4.0–4.5 m tree height and 0.6–0.8 m trunk height; 3~4 main branches that were 2.5–3 m long; main branch base angle of 70~75°; waist angle of 70~80°; tip angle of 65~70°; dry diameter of 0.4 m; and crown diameter of 3.22 m. The fruit was ovoid, fusiform, and oval with a regular medium size; the average fruit weight was 113.5 g per fruit. The fragrant pear tree selected in this paper had a height of H = 4.5 m, a stem height of h = 0.8 m, and a crown diameter of D = 3.6 m. The fruit on the fragrant pear tree were distributed at a ratio of 1:3:1 from top to bottom. To facilitate the indoor study, an equal-scale model of a fragrant pear tree was built, as shown in Figure 2.

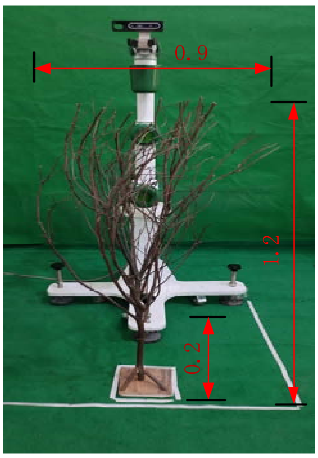

Figure 2. Indoor model of a fragrant pear tree.

2.2. Fragrant Pear Physical Properties

In 2020, the Xinjiang Uygur Autonomous Region Market Supervision Administration released the quality grading standard GDB65/T4295-2020 for Xinjiang Korla fragrant pear fruit. Accordingly, the quality of fragrant pears is divided into three standards: special grade, first grade, and second grade. In the orchard, we randomly selected 20 fruit trees, and on each tree, we randomly selected 10 fresh fragrant pears with no fruit surface defects that had normal fruit shape, fruit surface neatness, and fine skin. The physical parameters of the fragrant pears were measured using a balance scale with a range of 0.2–300 g and an accuracy of 0.01 g and zinc alloy digital display calipers with a range of 150 mm and a resolution of 0.01 mm. The specific data are shown in Table 1.

Table 1. Physical parameters of fragrant pears.

Grading Criteria	Individual Metrics	Quality m/g	Cross Axis Length Dha/mm	Vertical Axis Length Dva/mm
Premium	Maximum value	153.15	68.22	75.32
	Minimum value	122.11	59.35	66.77
	Average value	133.32	62.31	58.33
Level 1	Maximum value	121.36	60.11	71.99
	Minimum value	101.33	53.89	54.63
	Average value	109.21	57.36	62.36
Level 2	Maximum value	100.01	57.31	66.88
	Minimum value	96.38	54.11	52.35
	Average value	97.69	55.25	58.36

2.3. Selection of a Robotic Arm

Based on the actual situation, the robotic arm needs to be mounted on a mobile platform to carry out fragrant pear-picking between the rows of the orchard. Through the platform's movement around a fruit tree, the picking robot arm can achieve complete coverage of a fragrant pear tree. In order to save costs and achieve a multipurpose claw, the selected mechanical arm end of the claw diameter range should be between 52 and 75 mm, the payload should be 200 g or more. In addition, the workspace in the mobile platform at rest should be as large as possible to cover the fragrant pear tree canopy range to improve the efficiency of the mechanical arm picking. Fragrant pear orchards have a considerable fruit shade, a wide fruit distribution, complex growth environments, and many other conditions. Therefore, in order to successfully complete the task of fruit picking, the mechanical arm should have a simple structure and reliable efficiency. SLI is used as one of the indicators to evaluate the performance of a robotic arm and reflects the structural efficiency of the arm. It is defined as the ratio of the sum of the length of the robotic arm linkage to the cube root of the volume of the workspace reachable at its end [20].

$$L = \sum_{i=1}^{n} (a_i + d_i) \tag{1}$$

$$S = \frac{L}{\sqrt[3]{V}} \tag{2}$$

where a_i is the linkage length, d_i is the linkage offset, and V is the workspace reachable by the end-effector of the robot arm.

The smaller the sum of the robotic arm linkage, the larger the end-effector reachable space, i.e., the smaller the S, the more reasonable the robotic arm design, and the higher the robotic arm efficiency. The length and bias of each linkage in the robot arm are known, and the robot arm workspace space and robot arm performance indexes are analyzed according to the kinematic parameters of the robot arm using the Monte Carlo method, as shown in Figure 3.

The working space V of the robotic arm is spherical with a radius of 720 mm and a volume of 1.56×109 mm^3. When substituted into Equation (2), L is 980 mm, and S is 0.8507, which indicates that this robotic arm is suitable for the task of picking fragrant pear.

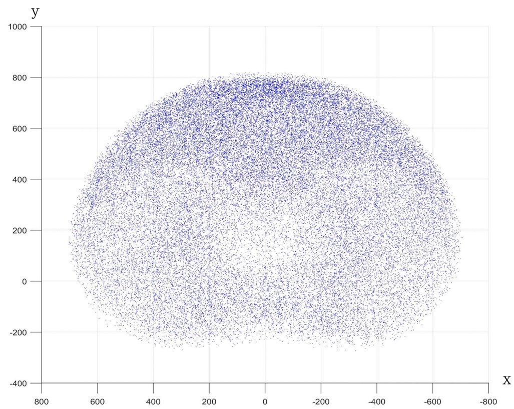

Figure 3. Manipulator workspace.

The six-axis picking robot arm has many advantages such as good flexibility, strong compatibility, and simple structure, and can meet the positioning requirements at any point in space. Thus, the arm can successfully complete the fruit-picking task in orchards with many conditions such as considerable fruit shade, a wide fruit distribution, and complex growth environments [21–29]. The ROCR6 robot arm has a compact structure and excellent servo performance. The angle detection of the joint torque motor uses 20,000 lines of incremental encoder, and the detection of the joint angle uses a 17-bit absolute encoder with an angle resolution of less than 0.001°. The repeat positioning accuracy of a single joint is better than 0.005°, and the repeat positioning accuracy of the robot arm is better than ±0.02 mm, which is easy to install and arrange. The end position and movement track can be controlled using monitoring software, which supports C language programming for setting. It also supports the transmission of target position signals through CAN bus and RS232 communication and has high-cost performance, making it suitable for small fragrant pear orchards for its application in fragrant pear picking. Considering these factors, the ROCR6 six-axis robot arm was selected as the working platform to study the fragrant pear-picking sequence. The structure is shown in Figure 4.

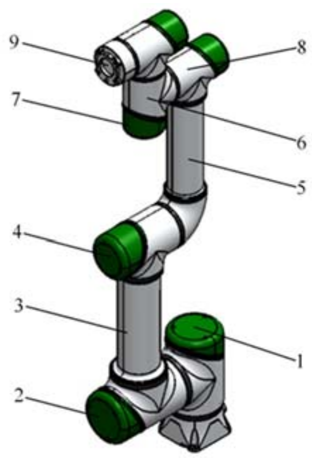

Figure 4. ROCR6-type six-axis robotic arm: 1. joint 1, 2. joint 2, 3. large arm, 4. joint 3, 5. small arm 6. joint 4, 7. joint 5, 8. joint 6, and 9. end flange coupling.

3. Horizontal Pre-Picking Points and Drop-Off Points

3.1. Horizontal Pre-Picking Points

The characteristics of the fragrant pear's delicate nature (i.e., pear shape and smooth skin) necessitate that the end of the robot arm actuator in proximity to the picking position must be gentle. Considering time and economic costs, the less time required for the robot arm to perform the task of picking, the lower the cost of picking. As a result, pre-picking points must be set up in the pre-picking stage of the robotic arm. In the orchard, the distance between the pre-picking point and the picking point is between 20 and 25 cm, considering obstacles such as tree branches. The indoor experimental site built in this study had a pre-picking point and picking point distance of 1–3 cm without considering obstacle avoidance. According to its characteristics, the principle of "big in big" is proposed, that is, a big step length approaching the fruit, a medium step length picking the fruit, and a big step length putting down the fruit [30]. The relationship between the angular velocity of its two joints is this:

$$V_1 = kV_2 \tag{3}$$

where V_1 is the large step joint angle velocity, V_2 is the angular velocity of the mid-step joint, and k is the scaling factor. In this paper, V_1 = 10, V_2 = 1, K = 10.

The initial pre-picking point, picking point, and drop-off point (the initial location for picking the next fragrant pear) are shown in Figure 5.

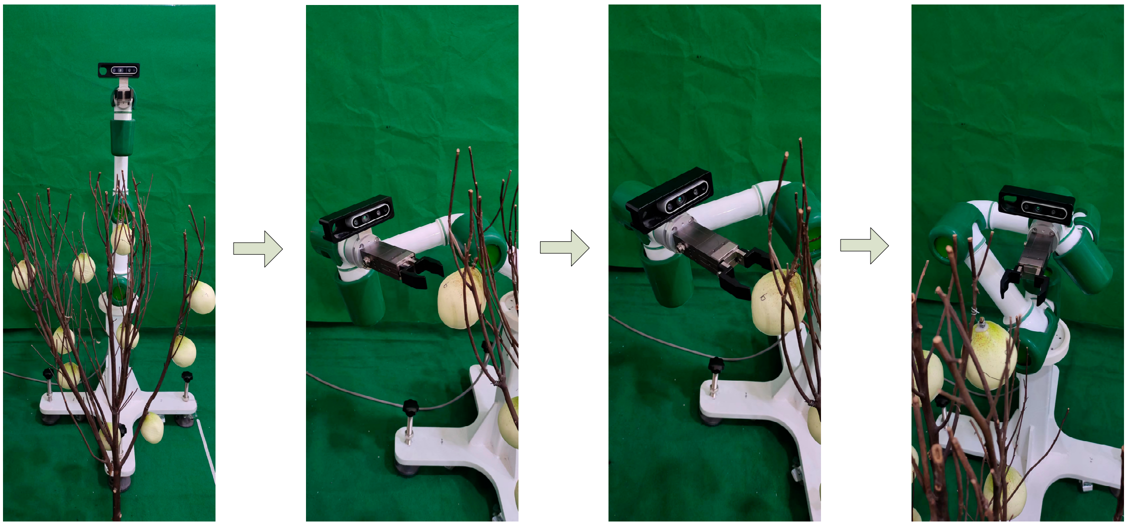

Figure 5. Fragrant pear-picking process.

3.2. Horizontal Drop-Off Point

The existing research on the drop-off point of the fruit-picking robotic arm is mainly divided into two kinds: The first is picking a fragrant pear and putting it into a storage box with a low posture. The second is the robotic arm itself carrying the guide fruit hose for uninterrupted picking. The low manner in which the pear is put into the storage box directly leads to an extended time of the picking task. In addition, when using the guide hose in the branches of a messy, fragrant pear tree to perform the picking task, it is difficult for the robot arm to avoid obstacles, which can easily cause damage to the robot arm. In response to this problem, the drop-off point can be set between the pear tree and the mechanical arm while ensuring that the force on the fragrant pear from dropping off to rolling down into the storage box is less than 40 N, which does not prevent the subsequent fragrant pear picking [31–35]. Using several experiments, the location of the drop-off point was determined to be 38.5 cm from the center of the robot arm base and 105 cm from the ground. At the drop-off point where the jaws release the fruit, the fragrant pear rolls down into the storage box through EPE material made of a telescopic guide tube, as shown in Figure 6.

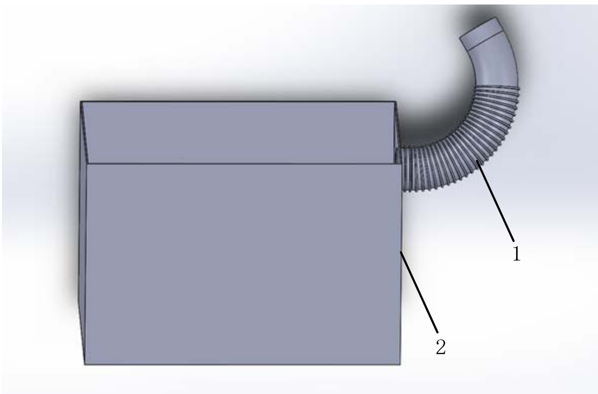

Figure 6. Fragrant pear storage device. 1. Fruit guide tube. 2. Storage box.

4. Fragrant Pear-Picking Order

The number of fragrant pears in the model tree was 5, 10, and 20, i.e., we obtained three sets of data for experimental validation of the picking sequence. The robot arm itself is built with an Intel Real Sense D435 camera, which uses the binocular calibration principle to calibrate the 3D coordinates of a fragrant pear.

4.1. Hybrid Ant Colony–Particle Swarm Algorithm

The TSP, or traveling salesman problem, which can be translated into a stretcher boy or traveling merchant problem, was first proposed by Euler to study the traveling rider problem. It was introduced by the RAND Corporation to the United States and gradually became a well-known and popular problem. The TSP problem can be simply understood as how a merchant who wants to do business in n cities can ensure that he passes through each city once and that the total path is the shortest. Given a weighted path graph M = (S, C), where S = 1, 2, . . ., n is the set of all vertices passing through the cities, C is the set of edges consisting of the vertices of each city connected to each other, and $D = \{d_{ij} \mid i, j \in C, d_{ij} \in R\}$ denotes the set of shortest circuits for the journeys between the cities. W (M) denotes the set of all urban paths with the objective function $G(A) = \sum_{1 \le i \le n-1} d_{v_i v_j} + d_{v_n v_1}$ $G(P) = \min_{P \in W(M)} G(P)$, which is the shortest path in the objective function [36]. In this study of fragrant pear picking, the relevant algorithms for solving TSP are cited to plan the shortest path when the robotic arm is working, and the picking order of fragrant pears is determined microscopically to increase the efficiency of the robotic arm and reduce the loss of each joint in the robotic arm.

The ant colony algorithm was proposed by the Italian scholar COLORNI in 1991 to simulate the optimization algorithm by observing the foraging behavior of ants [37], which is actually formed using the principle of positive feedback combined with heuristic algorithms. The subsequent ant colony tends to choose the route with the highest pheromone concentration content and then leaves the corresponding pheromone on this route as well, forming a positive feedback mechanism that makes the search results of the whole colony converge to the optimal solution. The specific formula is as follows:

(1) The probability of ant k earning from picking point i to picking point j at a given moment

$$P_{ij}^{(k)}(t) = \begin{cases} \frac{[\tau_{ij}(t)]^{\alpha}[\eta_{ij}(t)]^{\beta}}{\sum\limits_{s \in a_k} [\tau_{ij}(t)]^{\alpha}[\eta_{is}(t)]^{\beta}} & j \in a_k \\ 0 & \text{else} \end{cases} \tag{4}$$

where a_k is all the picking points available to the ant in the next step, $\tau_{ij}(t)$ is the amount of pheromone on the path at moment t, $\eta_{ij}(t)$ is the desired amount of pheromone on the path at moment t, α is a pheromone-inspired factor, and $\beta\beta$ is the expected pheromone heuristic factor.

(2) Heuristic factor

$$\eta_{ij} = \frac{1}{d_{ij}}$$

where d_{ij} is the distance between picking points (i, j).

(3) Pheromone calculation

$$\tau_{ij}(t+n) = (1-\rho)\tau_{ij}(t) + \Delta\tau_{ij} \tag{5}$$

$$\Delta\tau_{ij}(t) = \sum_{k=1}^{g} \Delta\tau_{ij}^{(k)} \tag{6}$$

$$\Delta\tau_{ij}^{(k)} = \begin{cases} \frac{Q}{L_K} & \text{ant passes through edge}(i,\ j) \\ 0 & \text{else} \end{cases}$$

where ρ is the trajectory persistence factor, g is the total number of ants, $\Delta\tau_{ij}{}^{(k)}$ is the pheromone left on the path from i to j in this loop, $\Delta\tau_{ij}$ is the increment of pheromones left on the path from i to j in this loop, Q is a constant, and $L_K$is the distance traveled by ant K.

The particle swarm algorithm was proposed by American scholars Kennedy and Eberhardt in 1995 as an intelligent optimization algorithm for group collaboration by observing the foraging behavior of bird flocks [38]. The core of the algorithm is the use of mutual collaboration and information sharing between individuals to arrive at an optimal solution. The theory is based on an individual in a flock of birds acting as a particle and giving that particle a memory. The specific formula is as follows:

(1) Initialization phase

$$X_i = (x_{i1}, x_{i2}, x_{i3}, \ldots, x_{iD})\ i = 1,2,3,\ldots,N$$

$$V_i = (v_{i1}, v_{i1}, v_{i1}, \ldots, v_{iD})\ i = 1,2,3,\ldots,N$$

where X_i is the ith particle position, V_i is the velocity of the ith particle, N is the total number of particles, and D is a D-dimensional search space.

(2) Update rate

$$v_{id}^{m} = \omega v_{id}^{m-1} + c_1 r_1 (pb_{id} - x_{id}^{m-1}) + c_2 r_2 (gb_d - x_{id}^{m-1})$$

where ω is an inertial constant, c_1 and c_2 are learning factors that regulate the learning step size, r_1 and r_2 are random functions with values in the range [0, 1], m is the m-th iteration, pb_{id} is the best position for particle i, and gb_d is the best position for the population.

(3) Update location

$$x_{id}^{m} = x_{id}^{m-1} + v_{id}^{k-1}$$

The ant colony algorithm and particle swarm algorithm have good performance in solving TSP-like problems such as combinatorial optimization, function optimization, fuzzy control, etc., but at the same time, there are many drawbacks.

The disadvantages of ACO algorithms include blindness, pheromone dependence, and difficulty in parameter selection, and the disadvantages of particle swarm algorithms include problem dependence, limitation of population size, and tendency to fall into a locally optimal solution. In contrast, the hybrid ant colony–particle swarm optimization algorithm can increase the diversity of particles in the particle swarm with the cross-mutation of particles with smaller fitness values while retaining the information of the excellent population. In doing so, the exchange of information between particles can be based on the pheromone of the ant colony algorithm and the global optimal particles in the particle swarm algorithm at the same time, which can avoid falling into a locally optimal solution and at the same time improve the convergence speed of the algorithm.

The algorithm is divided into two main steps: The first step uses the fast and global nature of the particle swarm algorithm to perform a coarse search over a large area, which is then iterated to produce a suboptimal solution. The second step uses the suboptimal solution derived from the particle swarm algorithm to initially distribute the pheromone matrix of the ACO algorithm to reduce the blindness of the ACO algorithm, thus reducing the search space and ultimately finding the optimal solution to this problem [39–41]. The specific formulation of the hybrid ant colony–particle swarm optimization algorithm is shown below:

(1) Ant location update

$$X_i(t+1) = X_i(t) + \Delta X_i(t)$$
$$\Delta X_i(t) = \eta * \Delta T_i(t) + \eta' * \Delta\eta_i(t)$$

where $X_i(t)$ is the position of ant i at time t, ΔX_i is the amount of change in the position of ant i, η is the pheromone importance factor, $\Delta T_i(t)$ is the amount of pheromone change, η' is the heuristic information importance factor, and $\Delta\eta_i(t)$ is the heuristic pheromone change.

(2) Pheromone update

$$T_{ij}(t+1) = (1-\rho) * T_{ij}(t) + \Delta T_{ij}$$

where $T_{ij}(t+1)$ is the concentration of pheromone in the path at t + 1, ρ is the pheromone volatility factor, and ΔT_{ij} is the amount of pheromone change.

The particle velocity and position are updated using the above equation. A flowchart showing the hybrid ant colony–particle swarm optimization algorithm is shown in Figure 7.

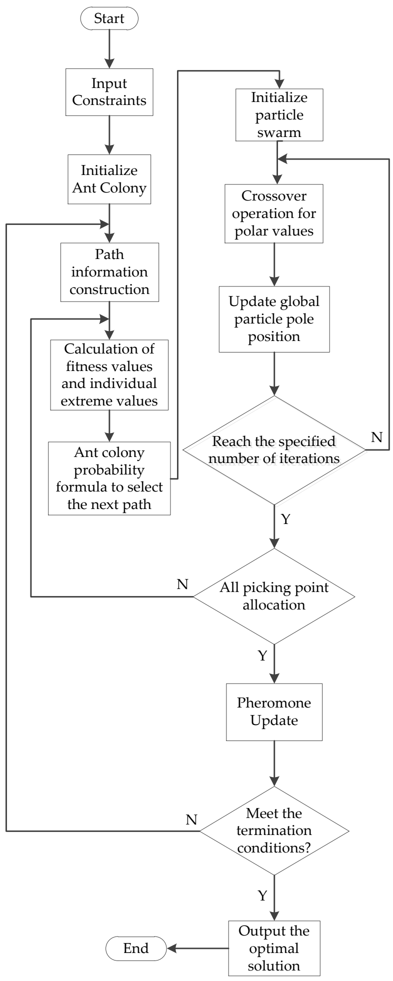

Figure 7. Flow chart showing the hybrid ant colony–particle swarm optimization algorithm.

The picking sequence that was planned using the hybrid ant colony–particle swarm optimization algorithm is shown in Figure 8.

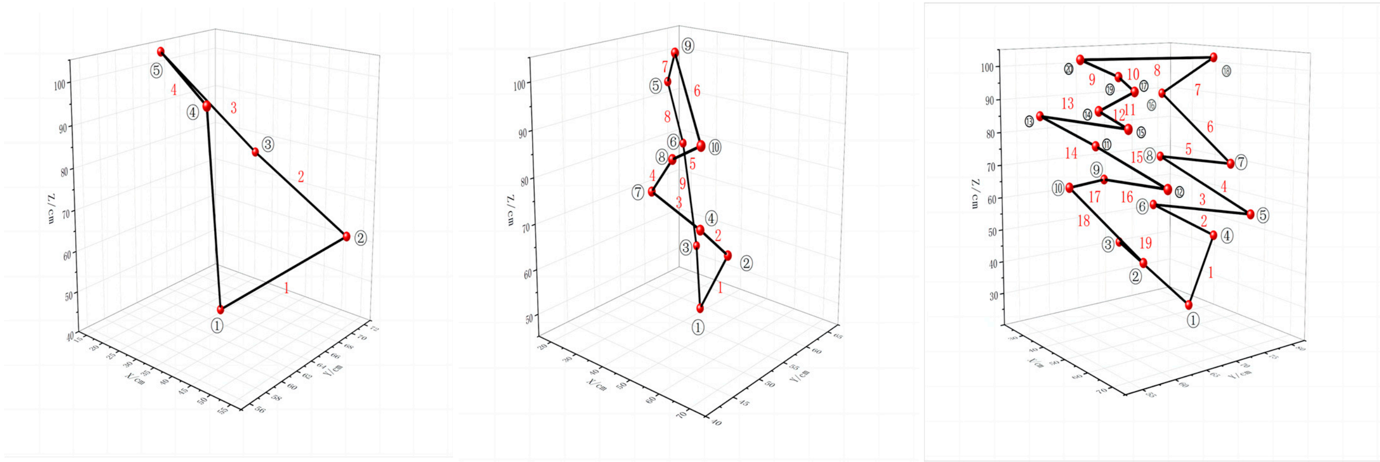

Figure 8. 5, 10, and 20 picking order for each group of balsam pears.

The distribution of numbered red spheres in the figure represents the coordinates of fragrant pears, and the red numbers indicate the order of picking. Figure 9 shows the Pucai converter metering socket that was used to detect the power, voltage, time, and electricity consumption of a robotic arm while using the hybrid ant colony–particle swarm optimization algorithm for picking three groups of fragrant pears. The time and energy consumed by the hybrid algorithm is shown in Table 2.

Figure 9. One 10A NFC cell phone communication Pucai converter metering socket.

Table 2. Average energy consumption and time consumption of hybrid algorithms.

Number of Fragrant Pears	Average Energy Consumption of the Hybrid Algorithm (/w·h)	Average Time Taken by the Hybrid Algorithm (s)
5	1.415	98.52
10	2.863	180.36
20	3.731	260.41

4.2. Multiple Weighting Method

In contrast to the intuitiveness of the hybrid algorithm applied to robotic picking, the principle of minimum energy consumption treats each joint of the robotic arm as a motion unit, and the power of each joint of the robotic arm is used as a weighting factor to calculate the optimal position. In the past, weighted studies of the joints in the picking robot arm considered continuous picking, that is, the robot arm picked the first fragrant pear from the initial position and then immediately went to the next fragrant pear position while the fragrant pear rolled down to the storage box through the hose. The hose is often attached to the robot arm linkage and moves with the robot arm. In the picking process, the end-effector shuttles between the branches of the pear tree to perform the picking task. To a certain extent, the existence of the hose reduces energy loss while the robotic arm performs the task of picking and saves picking time. However, fragrant pear tree branches often cause the hose to fall, resulting in the robotic arm joints being overloaded with power, making it difficult for the robotic arm to recover from damage. Utilizing a hose for the post-picking transfer of fragrant pears increases both the difficulty of avoiding obstacles when the robotic arm performs the picking task and the inability to grade the quality of the fragrant pears, thereby increasing the economic cost.

In response to the problems associated with continuous picking, the multiple weighting method removed the guide fruit hose and increased the fragrant pear placement point. The fragrant pear quality standard is divided into three levels, and the placement point position can be set to three. The grade of a fragrant pear can be automatically calibrated using contour detection, Haar + AdaBoost target detection technology, and pressure sensors installed in the mechanical gripper, according to the previously mentioned fragrant pear grading standards, with the help of the Intel RealSenseD435 camera on the robotic arm. The implementation of the picking task through the different drop-off points directly leads to fragrant pear grading, eliminating the manual sorting link and saving economic costs. However, the establishment of three drop-off points makes the computational volume grow geometrically. In order to facilitate the comparison between energy consumption and the picking order planned using the hybrid algorithm mentioned above, this paper only sets up a fixed drop-off point and utilizes the multiple weighting method to plan the picking order for three groups of fragrant pears. A flowchart illustrating the multiple weighting method is shown in Figure 10.

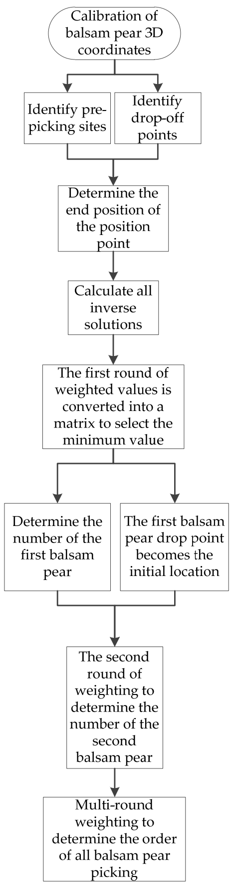

Figure 10. Flowchart showing multiple weighting method.

The six joint motors in the six-axis robot arm are divided into two main parts. The first part is for joints 1 and 2, using RJSII-17 joint modules rated at 200 W; the second part is for joint 3, using RJSII-14 joint modules rated at 118 W; and the last part is for joints 4, 5, and 6, using RJS14S joint modules rated at 59 W. The specific data are listed in Table 3.

Table 3. Power and weighted values of each joint motor.

Joint	1	2	3	4	5	6
Joint power/(W)	200	200	118	59	59	59
Weighting factor	0.20	0.20	0.118	0.059	0.059	0.059

4.2.1. The First Fragrant Pear Picking Location

The energy minimization principle was used to plan the fragrant pear-picking sequence. The objective function is

$$f = \sum_{i=1}^{a} \omega_i J_i = \sum_{i=1}^{a} \sum_{j=1}^{b} \omega_i \left| \theta_{i,j} - \theta_{i,j+1} \right|$$

where a is the number of robotic arm joints (a = 6), b is the number of fragrant pears, ω_i is the weight coefficient of each joint of the robot arm, and θ_{ij} is the joint angle of the ith joint of the robot arm when picking the jth fragrant pear.

According to the analysis of the working characteristics of the robotic arm and the planning of the fragrant pear-picking sequence, the minimum energy consumption method based on multiple weighting is proposed by combining the above energy consumption objective function with the addition of graded drop-off points. Based on the multiple weighting method, the objective function of the six-axis robotic arm for the fragrant pear-picking sequence is planned as:

$$f = \min\left(\left|\theta_c - \theta_y\right| w_i + \left|\theta_y - \theta_z\right| w_i + \left|\theta_z - \theta_t\right| w_i \right)$$

where θ_c is the initial angle of the robot arm (0, 0, 0, 0, 0, 0, 0), θ_y is the robot arm pre-picking point, θ_z is the robot arm's picking point, and θ_t is the robot arm drop-off point. Without considering the singular position of the robot arm, the end poses of the robot arm at each point can be considered to have eight sets of inverse solutions. The first weighting is from the initial position to the pre-picking point position, which is weighted to give 64 results. The second weighting is from the pre-picking point to the picking point position, which is weighted to give 64 $\times$ 8 sets of weights. The third weighting is from the picking point position to the drop-off point position, which is weighted to give 64 $\times$ 8 $\times$ 8 sets of weights. That is, each fragrant pear has 4096 sets of weights. The group with the smallest weighted value in all fragrant pears is the joint angle at each location point when picking fragrant pears. The group with the smallest weighted value of all the fragrant pears is the joint angle of the robotic arm at each position point when picking fragrant pears, and the order in which the first fragrant pears are picked is thus determined.

4.2.2. The Picking Order of the Subsequent Fragrant Pear

After the first fragrant pear reaches the drop-off point, in order to reduce the joint transformation angle and reduce the amount of calculation, the joint angle position at this moment is the initial joint angle, and then the operation stated above is repeated. The first weighting is from the initial position to the pre-picking point position, which is weighted to yield 1 $\times$ 8 sets of weighted values. The second weighting is from the pre-picking point to the picking point position, which is weighted to yield 8 $\times$ 8 sets of weighted values. The third weighting is from the picking point position to the drop-off point position, which is weighted to yield 8 $\times$ 8 $\times$ 8 sets of weighted values. That is, there are 512 sets of weighted values in picking each fragrant pear, disregarding the singular position. The smallest group in all the weighted values is the joint angle of this fragrant pear at each location point. Then, the second picking order of fragrant pears can be determined. This operation is repeated in the subsequent fragrant pear picking orders to finally determine the picking order of all fragrant pears.

5. Experimental Analysis

5.1. Order of Fragrant Pear Weights

Tables 4–6 show the weights and picking order of the three groups of fragrant pears, respectively.

Table 4. Picking sequence and weight values for 5 fragrant pears.

Picking Order	Fragrant Pear Number	Total Weight
1	5	100.65
2	2	102.46
3	3	102.72
4	1	134.14
5	4	139.28

Table 5. Picking sequence and weight values for 10 fragrant pears.

Picking Order	Fragrant Pear Number	Total Weight
1	2	45.78
2	8	56.97
3	7	70.30
4	4	81.49
5	10	104.03
6	5	107.19
7	3	136.44
8	9	141.64
9	6	148.27
10	1	166.27

Table 6. Picking sequence and weight values for 20 fragrant pears.

Picking Order	Fragrant Pear Number	Total Weight
1	16	87.36
2	19	87
3	4	87.69
4	13	105.14
5	15	111.43
6	17	113.37
7	3	113.54
8	8	115.19
9	18	120.07
10	7	127.28
11	2	135.52
12	20	135.52
13	6	139.33
14	9	142.25
15	11	146.68
16	14	146.89
17	12	152.33
18	5	164.72
19	1	172.93
20	10	186.28

From Figures 11–13, it can be seen that when picking a fragrant pear, the range of change in each joint angle in the robotic arm is basically between [−150, 150] in the robotic arm movement range of [−180, 180]. This indicates that a number of weighting regulations delineate the picking order, which reduces energy consumption and ensures the success rate of picking fragrant pears. In accordance with the order of the weighted value from small to large, the multiple weighting method is used in each round of weighted values to select the smallest weighted value of the fragrant pear as the target of this picking. The weighted value of one round is not necessarily smaller than the weighted value of the next round. As listed in Table 6, the picking order of fragrant pears numbered 16, 19, 9, and 11 is not in accordance with the overall size of the weights, but rather the smallest value of the weights in a round of weighting.

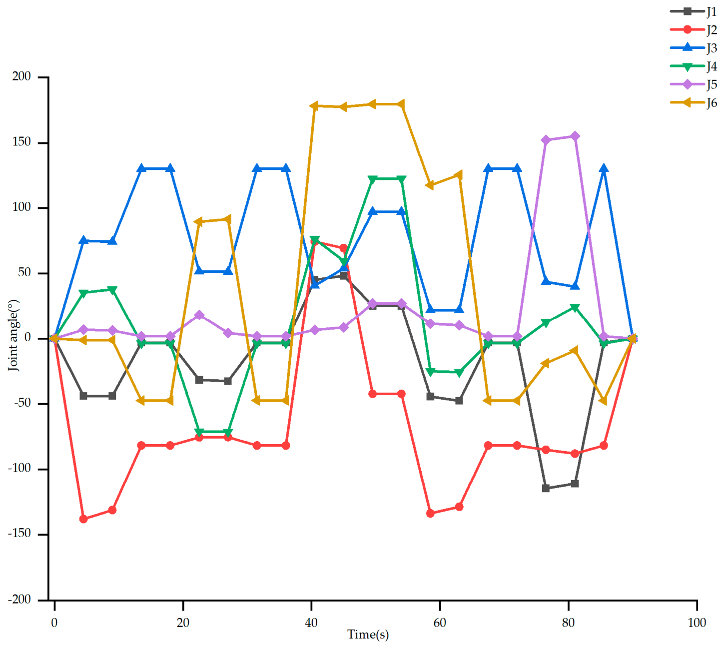

Figure 11. Angle of each joint when the number of picked fragrant pears is 5.

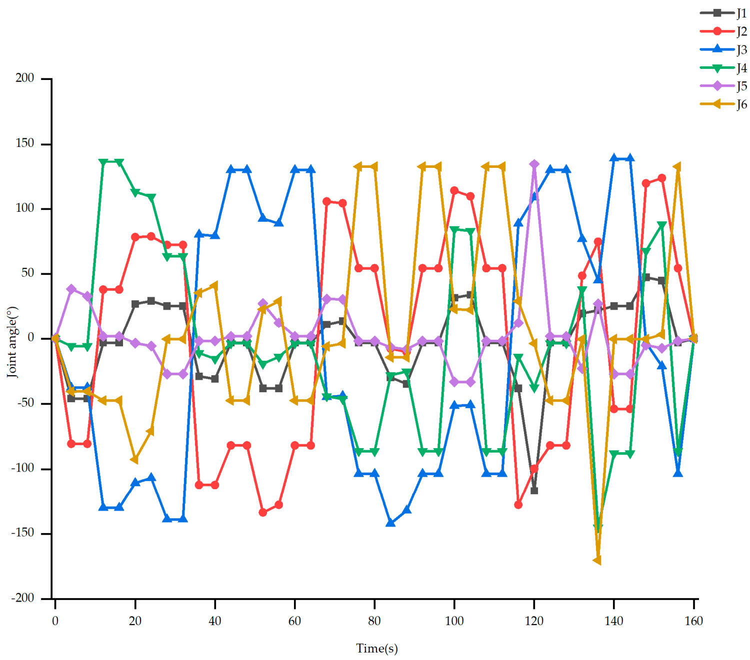

Figure 12. Angle of each joint when the number of picked fragrant pears is 10.

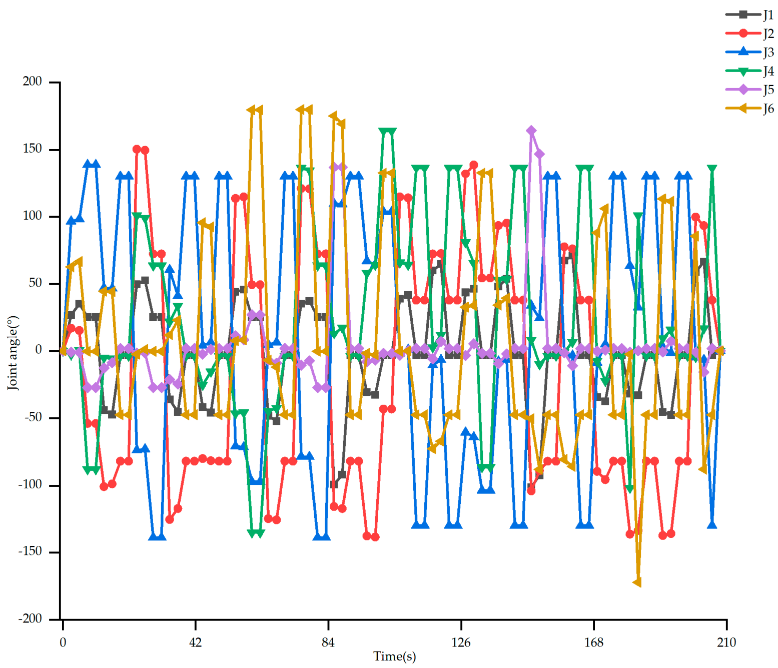

Figure 13. The angle of each joint when the number of picked fragrant pears is 20.

5.2. Time and Energy Consumption during Harvesting

From Tables 7 and 8, it can be seen that, relative to the hybrid algorithm, the multiple weighting method significantly reduces the average energy consumption and average time consumption of the robotic arm. The percentage reduction in both is almost equal, which fully demonstrates the superiority of the multiple weighting method in planning the fragrant pear-picking sequence.

Table 7. Average energy consumption time of two methods.

Number of Fragrant Pears	Average Energy Consumption of the Hybrid Algorithm (/w·h)	Multi-Weighted Method Average Energy Consumption (/w·h)	Percentage Reduction
5	1.515	1.354	10.627%
10	2.663	2.235	16.072%
20	3.731	2.820	24.417%

Table 8. Average time consumption of the two methods for picking fragrant pears.

Number of Fragrant Pears	Average Energy Consumption of the Hybrid Algorithm (/w·h)	Multi-Weighted Method Average Energy Consumption (/w·h)	Percentage Reduction
5	98.32	86.51	11.988%
10	170.36	145.78	14.428%
20	260.41	201.66	22.561%

6. Robotic Arm Life Calculation

Determining the loss of joint modules not only facilitates the maintenance and servicing of each joint in the robot arm but also indirectly reduces the economic cost, which is conducive to the wide range of use for fruit-picking robot arms.

The rotation of the robotic arm joints is performed by a combination of servo drives, frameless torque motors, harmonic reducers, optical encoders, absolute encoders, and relay holding brakes. Among them is a frameless torque motor that acts as a drive motor. The motor itself does not carry bearings; by adding a reducer and bearings inside it, the wear and tear of the inner and outer rotors inside the reducer directly affects the service life of the robot arm. The robotic arm joint loss is determined by calculating the cumulative change in the angle of each joint during robotic arm picking.

$$S = \frac{\sum|\theta_m - \theta_c|}{\alpha} \times 100\% \quad (7)$$

where S is the loss ratio, θ_m is the initial joint angle, θ_c is the end-position joint angle, and α is the rotation angle within the life of the inner and outer rotors.

The lifetime of both the inner and outer rotors of each joint in the robot arm is 1000 h, and the rated speeds of the inner and outer rotors are 1000 rpm and 30 rpm, respectively, i.e., the maximum rotation angles of the inner and outer rotors are 2.16×10^{10} and 6.48×10^{8}, respectively, during its service life. By dividing the accumulation of each joint angle by the maximum rotation angle when picking fragrant pears, the loss of the robot arm for this picking task is determined, as listed in Table 9.

Table 9. Internal and external rotor loss ratio.

Joints of the Robot Arm	Outer Rotor Loss Ratio	Inner Rotor Loss Ratio
1	$5.394 \times 10^{-4}\%$	$1.618 \times 10^{-2}\%$
2	$8.488 \times 10^{-4}\%$	$2.546 \times 10^{-2}\%$
3	$1.532 \times 10^{-3}\%$	$4.596 \times 10^{-2}\%$
4	$1.263 \times 10^{-3}\%$	$3.763 \times 10^{-2}\%$
5	$3.807 \times 10^{-4}\%$	$1.142 \times 10^{-2}\%$
6	$1.434 \times 10^{-3}\%$	$4.302 \times 10^{-2}\%$

After the subsequent execution of the task of picking fragrant pears, the loss of the rotor is obtained using the accumulation of the loss ratio, which facilitates the subsequent maintenance and repair of the robot arm, thus extending the service life of the robot arm.

7. Summary

In this paper, a multiple-weighting method is proposed to address the problem of multiple fragrant pear-picking sequences. The method is based on the principle of minimum energy consumption and considers the loss of each joint when the robotic arm performs the picking task. Compared with the picking sequence planned for a similar six-axis robotic arm installed with a fruit-guiding hose using the principle of minimum energy consumption in the literature [16,19], the energy consumption and time consumed when using the multiple-weighting method are almost unchanged when picking 5 and 10 fragrant pears, respectively. In addition, the multiple-weighting method removes the fruit-guiding hose, which prevents the robotic arm from being damaged. The additional drop-off point is conducive to the integration of the subsequent picking and grading of fragrant pears, in line with the concept of automation of the whole process of picking. Determining the minimum weights reduces the loss of each joint in the robotic arm, reduces the cost of use, and fully demonstrates the superiority of the multiple-weighting method for planning a fragrant pear-picking sequence.

Author Contributions: Conceptualization, W.M. and Z.Y.; methodology, W.M.; software, D.L.; validation, Y.X. and X.Y.; formal analysis, Z.Y.; investigation, X.Y.; resources, H.T.; data curation, W.M.; writing—original draft preparation, X.Q.; writing—review and editing, W.M.; visualization, Y.L.; supervision, X.Y.; project administration, X.Y.; funding acquisition, Y.L. All authors have read and agreed to the published version of the manuscript.

Funding: This research received no external funding.

Institutional Review Board Statement: This study had no ethical implications and did not require ethical approval.

Data Availability Statement: Data that cannot be used publicly due to privacy restrictions.

Conflicts of Interest: The authors declare no conflict of interest.

References

1. Du, J.H. Korla Fragrant Pear: Why the National Pear Category "C"—Xinjiang Agricultural Advantageous Characteristic Industry Cluster Series of Reports of the Second Shi Guan Yun/Xinjiang Daily News 2023. Available online: http://nynct.xinjiang.gov.cn/xjnynct/c113576/202302/792239b2cb484a2592142a3ea5f26bf4.shtml (accessed on 25 June 2023).
2. Guang, X.M. Study on the Variation of Fruit Quality during Harvesting and Storage Period of Korla Fragrant Pear. Master's Thesis, Tarim University, Alar, China, 2018; pp. 3–4.
3. Liu, Y.K.; Gao, H.L.; Zhang, J. Design and visual algorithm improvement of an apple picking system based on an open source project. *Jiangsu Agric. Sci.* **2019**, *47*, 187–192.
4. Zhu, W.Q. Electrical control system of a picking manipulator based on a PLC and particle swarm algorithm. *Agric. Mach. Res.* **2021**, *43*, 238–241+246.
5. Luo, L.F.; Tan, Y.L.; Lu, Q.H. Research progress on visual cognition and its actuator for fruit anti-bump damage picking. *J. Hebei Univ. Sci. Technol.* **2018**, *39*, 204–213.
6. Zhang, S.S.; Wang, Z.Y.; Chen, L.P. MatLab-based multi-objective kiwifruit non-destructive picking path planning. *Agric. Mech. Res.* **2019**, *41*, 18–23.
7. Wang, B.X.; Wang, S.A.; Yu, D.H. Fruit cluster identification and picking order planning based on selective attention mechanisms. *J. Agric. Mach.* **2016**, *47*, 1–7.
8. Liu, F. Research on citrus picking sequence planning based on an improved ant colony algorithm. *Inf. Comput. (Theor. Ed.)* **2022**, *34*, 44–46.
9. Yuan, Y.W.; Zhang, X.C.; Hu, X.A. Optimization algorithm and simulation implementation for apple picking path planning. *J. Agric. Eng.* **2009**, *25*, 141–144.
10. Tang, Z.L. Research on Motion Planning of Citrus Picking Robot Arm. Master's Thesis, Sichuan Agricultural University, Ya'an, China, 2022; pp. 71–83.
11. LI, Y.T. Vision Detection and Positioning Technology for Tea Picking Robots. Ph.D. Thesis, Zhejiang University of Technology, Hangzhou, China, 2022; pp. 84–87.
12. Ling, J.S. Citrus Picking Path Planning and System Implementation Based on 3D Point Cloud Model. Master's Thesis, Huazhong Agricultural University, Wuhan, China, 2022; pp. 52–57.
13. Wan, S.M. Research on the Path Planning Method of a Tea-Picking Robotic Arm with Time-Optimal Control. Master's Thesis, Anhui Agricultural University, Hefei, China, 2022; pp. 46–52.
14. Feng, X.P. Optimal Configuration Strategy for Multiple Cartesian Coordinate Parallel Fruit Picking Robotic Arms. Master's Thesis, Sichuan Agricultural University, Ya'an, China, 2022; pp. 23–31.
15. Niu, Y.D. Research on the Evaluation Method of Picking Convenience of a Robotic Arm for Fruit Picking Robot. Master's Thesis, Sichuan Agricultural University, Ya'an, China, 2021; pp. 46–71.
16. Zhang, Z. Study on the Picking Pose and Sequence of the Citrus Picking Robot. Master's Thesis, Chongqing University of Technology, Chongqing, China, 2018; pp. 55–59.
17. Teng, J.Y. Motion and Task Planning of a Six-Degree-of-Freedom Picking Robot Arm. Master's Thesis, Chongqing University of Technology, Chongqing, China, 2017; pp. 35–43.
18. Gu, B.X. Research on an Intelligent Mobile Fruit Picking Robot System. Ph.D. Thesis, Nanjing Agricultural University, Nanjing, China, 2012; pp. 64–67.
19. Wang, Y. Key Technology Research on Bite-Type End-Effectors for Citrus Picking Robots. Ph.D. Thesis, Chongqing University, Chongqing, China, 2019; pp. 124–127.
20. Zhao, Z.Y.; Xu, Z.B.; He, J.P.; He, H.; Xu, C. Optimization of a 9-degree-of-freedom super-redundant tandem robotic arm configuration based on workspace analysis. *J. Mech. Eng.* **2019**, *55*, 51–63.
21. Zhang, W.X.; Zhang, B.Y.; Gong, Y.; Ren, N. Current status and prospects of research on robotic arms for fruit and vegetable picking. *Chin. J. Agric. Chem.* **2022**, *43*, 232–237+244.
22. Zhang, P.; Tang, Q.Y.; Chen, L.F.; Qin, C.L.; Wang, L.Y. Analysis of the current situation and progress of fruit and vegetable picking robot research. *South. Agric. Mach.* **2023**, *54*, 9–12.
23. Wang, S.Y.; Niu, C.Q.; Li, Z.; Shi, W.J.; Fan, G.J. Current status and trends of research on typical fruit and vegetable picking robots. *Xinjiang Agric. Mech.* **2021**, *6*, 14–17+21.
24. Wu, R.D.; Chen, T.C.; Zhang, S.A.; Zhu, L.X. Research progress of key technology for fruit and vegetable picking robots. *Mechatron. Eng. Technol.* **2021**, *50*, 128–132.
25. Jiang, X.P.; Xu, C.; Liu, F.B.; Wu, Y.F.; Wu, Y.F.; Xue, P.K. Application and development of robotic systems for fruit and vegetable picking. *Mod. Agric. Equip.* **2021**, *42*, 2–8+13.
26. Ao, M.Y. Analysis of the research status and countermeasures of fruit and vegetable picking robots. *Equip. Manuf. Technol.* **2019**, *3*, 128–131.

27. Li, Z.Y.; Yuan, X.J.; Wang, C.Y. A review on structural development and recognition-localization methods for end-effectors of fruit-vegetable picking robots. *Int. J. Adv. Robot. Syst.* **2022**, *19*, 3. [CrossRef]
28. Seol, J.; Lee, S.; Son, H.I. A Review of End-effectors for Fruit and Vegetable Harvesting Robots. *J. Korea Robot. Soc.* **2020**, *15*, 2. [CrossRef]
29. Xu, F. The Design of Six-DOF Fruit and Vegetable Picking Robot Based on Off-line Programming System. *J. Adv. Oxid. Technol.* **2018**, *21*.
30. Liu, D. Optimization of a Motion Planning Algorithm for a Citrus Picking Robot Arm in a Non-Structural Environment. Master's Thesis, Chongqing University of Technology, Chongqing, China, 2022; pp. 54–56.
31. Jiang, X.; Zeng, Y.; Liu, Y.; Zhang, Q.W.; Liao, J.A. Study on the impact damage pattern of Korla fragrant pear during picking and storage. *J. Tarim Univ.* **2023**, *35*, 99–104.
32. Li, X.L. Study on the Characterization Method of Static Pressure Damage to Korla Fragrant Pear. Master's Thesis, Tarim University, Xinjiang, China, 2022; pp. 14–16.
33. Yang, Y.X.; Yu, S.H.; Li, X.L.; Zhang, H.; Xiao, A.L.; Liu, Y.; Su, G.D. Study on the effect of different picking periods on static pressure damage to Korla fragrant pear. *Packag. Food Mach.* **2021**, *39*, 6–11.
34. Ma, R. Study on geometrical physical parameters and picking extrusion factors of Korla fragrant pear. *Agric. Mech. Res.* **2022**, *44*, 152–157.
35. Yang, Y.X. Hydrostatic Damage Mechanism and Quantitative Evaluation of Korla Fragrant Pear. Ph.D. Thesis, Tarim University, Xinjiang, China, 2021; pp. 16–20.
36. Wang, C.; Li, J.; Li, B. An improved hybrid ant colony and particle swarm algorithm for solving the traveler problem. *Comput. Simul.* **2016**, *33*, 274–279.
37. Colorni, A.; Dorigo, M.; Maniezzo, V. Distributed optimization by ant colonies. In Proceedings of the First European Conference on Artificial Life, Paris, France, 11–13 December 1991; pp. 134–142.
38. Eberhart, R.; Kenned, J. A new optimizer using particle swarm theory, Micromachine and Human Science. In Proceedings of the MHS'95, Proceedings of the Sixth International Symposium on Micro Machine and Human Science, Nagoya, Japan, 4–6 October 1995; pp. 39–43.
39. Min, K.X.; Ge, H.W.; Zhang, Y.; Liang, Y.C. A hybrid algorithm based on ant colony and particle swarm optimization for solving TSP problems. *J. Jilin Univ. (Inf. Sci. Ed.)* **2006**, *4*, 402–405.
40. Zhang, Y.; Shu, J. A hybrid algorithm based on ant colony and particle swarm optimization for solving TSP problems. *China Sci. Technol. Inf.* **2008**, *2*, 260–261.
41. Li, H.; Zhang, P.; Ma, C.; Zhao, J.; Shi, Y.; Jiang, X.B.; Yu, J.S. Optimization of the lateral force balance of a PDC drill bit based on the ant colony particle swarm hybrid algorithm. *Drill. Technol.* **2009**, *32*, 58–60+116.